Journal of Molecular Liquids 269 (2018) 203–210

Contents lists available at ScienceDirect

Journal of Molecular Liquids

journal homepage: www.elsevier.com/locate/molliq

Carbamate-bearing surfactants: Micellization, solubilization, and biological activity

Alla B. Mirgorodskaya [a,b,*], Rushana A. Kushnazarova [a], Svetlana S. Lukashenko [a], Alexandra D. Voloshina [a], Oxana A. Lenina [a], Lucia Ya. Zakharova [a,b], Oleg G. Sinyashin [b]

[a] Arbuzov Institute of Organic and Physical Chemistry, FRC Kazan Scientific Center of RAS, 8, ul. Arbuzov, Kazan 420088, Russian Federation
[b] Kazan National Research Technological University, 68, ul. K. Marx, Kazan 420015, Russian Federation

ARTICLE INFO

Article history:
Received 11 May 2018
Received in revised form 8 July 2018
Accepted 1 August 2018
Available online 03 August 2018

Keywords:
Carbamate-bearing surfactants
Aggregation
Solubilization
Antimicrobial activity

ABSTRACT

Herein novel cationic carbamate-bearing surfactants have been synthesized and characterized as effective building blocks for the development of polyfunctional nanosystems showing solubilizing, antimicrobial and membrane-tropic activity. For this purpose aggregation behavior of the surfactants has been evaluated, with the structure of head group and hydrophobicity varied. Their concentration and temperature ranges of micelle formation have been determined through tensiometry and conductometry: critical micelle concentration, Krafft point and adsorption parameters at the interface have been quantified. Solubilization of hydrophobic probes (Orange OT and pyrene) has been employed to determine aggregation numbers, evaluate solubilization capacity of micelles, and characterize micropolarity in the localization site of the probe. The value of LD_{50} of the carbamate-bearing surfactants has been determined (mice, intraperitoneal administration). It has been shown that the surfactants can be related to the class of moderately toxic compounds. Investigation of antimicrobial properties of carbamate-bearing surfactants has determined their significant antibacterial and antifungal activity against *Staphylococcus aureus*, *Escherichia coli*, *Bacillus cereus*, *Trichophyton mentagrophytes*, and *Candida albicans*.

1. Introduction

Amphiphilic compounds are mainstream as building blocks for the design of supramolecular systems showing high surface activity and solubilizing effect and act as effective nanocontainers and nanoreactors, which facilitate the administration of hydrophobic drugs into living and plant objects [1–4]. Possibilities of the employment of these substances in biotechnologies, pharmacology, and medicine make requirements of the properties of new amphiphiles, such as high performance under mild conditions and in the low concentration range, low toxicity, and the ability to overcome biological barriers, ability of multicharged interactions with loads on the one hand and biospecies on the other, morphological lability responsible for controlled structural behavior and binding/release behavior. Based on these criteria, new classes of amphiphilic compounds were synthesized and characterized in the past decade, with cationic surfactants received much attention. The latter is due to such properties of cationic amphiphiles as affinity to cell membranes and biopolyanions, e.g. DNA. Dicationic surfactants with low aggregation threshold [5–7]; degradable surfactants, which are capable of destruction under particular conditions [8–10]; and the surfactants containing fragments of natural compounds, which is critical to the increase in their biocompatibility [11–14], can be emphasized among them. Compounds containing urethane residue (organic carbamates) answer many of the above listed criteria, and therefore are of high practical importance. In particular, they can undergo of hydrolytic cleavage under physiological conditions [15–17]. When employed as carriers, they correspond to the criterion of biodegradability and can release active molecules after overcoming biological barriers involving blood brain barrier, which sets them apart from other cationic surfactants [18,19]. It should be noted that carbamate-bearing molecules play an important role in modern drug discovery and medicinal chemistry. Organic carbamates (or urethanes) are structural elements of many approved therapeutic agents. One example is that the simplest representative of this class of compounds, namely, ethyl carbamate, forms the basis for the drug urethane, which is used as sedative and tranquilizer, as well as anticonvulsant in children clinics. Ritonavir antiviral drug is successfully used along with other drugs for HIV/AIDS and virus hepatitis C therapy [20–23]. Proserin and biserin drugs, where urethane fragment is combined with quaternized nitrogen atom, can reversibly block cholinesterase [24,25]. They are effective muscle relaxants of peripheral action and are employed in therapy of myasthenia, motor impairment after brain injury, as well as in the recovery period after meningitis, poliomyelitis, encephalitis, and paralysis. Meanwhile, despite the high biotechnological opportunity little information is available on the amphiphilic analogues of these compounds;

* Corresponding author at: 8, ul. Akad. Arbuzov, Kazan 420088, Russian Federation.
E-mail address: mirgorod@iopc.ru (A.B. Mirgorodskaya).

https://doi.org/10.1016/j.molliq.2018.08.007
0167-7322/

it would be anticipated that the introduction of lipophilic substituents could facilitate drug transport. To compensate this, herein, a series of new alkylammonium cationic surfactants containing urethane fragment with a varying length of hydrocarbon tail and the structure of head group was synthesized and characterized. Formulae of the compounds are given below:

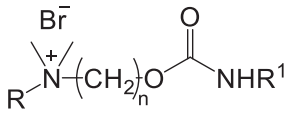

$14Q^+-2-Ur-4$: R = $C_{14}H_{29}$, R^1 = C_4H_9, *n* = 2; **$16Q^+-2-Ur-4$:** R = $C_{16}H_{33}$, R^1 = C_4H_9, n = 2; **$18Q^+-2-Ur-4$:** R = $C_{18}H_{37}$, R^1 = C_4H_9, n = 2; **$16Q^+-2-Ur-2$:** R = $C_{16}H_{33}$, R^1 = C_2H_5, n = 2; **$16Q^+-3-Ur-4$:** R = $C_{16}H_{33}$, R^1 = C_4H_9, *n* = 3.

2. Materials and methods

2.1. Materials

Commercially available Orange OT, pyrene, dipalmitoylphosphatidylcholine (DPPC), dimethylaminoethanols, hexadecyl bromides, butyl isocyanate, ethyl isocyanate, diazobicyclooctane (DABCO) (Sigma, 99%) were used without preliminary purification. All solutions were prepared with double-distilled water purified by Direct-Q 5 UV apparatus; the water resistivity was 18.2 MΩ·cm at 25 °C. Experimental temperatures were maintained at 25 ± 0.1 °C, unless otherwise indicated. All experiments were accurate within 4%.

2.2. Syntheses

The carbamates under study are prepared by the reaction of alkylammonium surfactant containing hydroxyethyl (or hydroxypropyl) substituent at head group with butyl isocyanate (or ethyl isocyanate) using DABCO as a catalyst. The scheme of the process and synthetic details are given on the example of the synthesis of N-[2-((butylcarbamoyl)oxy)ethyl]-*N*,*N*-dimethylhexadecaneammonium bromide (**$16Q^+$-2-Ur-4**) (see Scheme 1):

1 stage. Dimethyl(2-hydroxyethyl)hexadecylammonium bromide has been obtained through the reaction of dimethylaminoethanols and hexadecyl bromides in accordance with [26].

2 stage. The mixture of 3 g (0.0076 mol) of dimethyl(2-hydroxyethyl)hexadecylammonium bromide and 2.26 g (0.022 mol) of butyl isocyanate in 20 mL of acetonitrile was stirred in the flask equipped with a reflux condenser for 2 h at 55 °C. A total of 0.01 g (0.09 mmol) of 1,4-diazabicyclo[2.2.2]octane was used as catalyst. Upon completion of the reaction, volatile components were removed under vacuum. Dry residue was recrystallized twice from ethylacetate and dried under vacuum up to a constant weight; yield was 2.45 g (65%); mp 73–75 °C. The structure of the compounds was confirmed by elemental analysis, ESI mass spectrum, IR- and NMR-spectroscopy data.

N-[2-((butylcarbamoyl)oxy)ethyl]-*N*,*N*-dimethyltetradecaneammonium bromide (14Q^+-2-Ur-4) Yield 65%, mp 58–59 °C. IR spectrum, (KBr), *ν*, cm^{-1}: 3236, 2921, 2853, 1720, 1526, 1471, 1375, 1246, 1140, 1061, 975, 947, 721. ^{1}H NMR spectrum ($CDCl_3$, δ, ppm, *J*/Hz): 0.85–1104 m [6H, {N(H)$CH_2CH_2CH_2\underline{CH_3}$ + $N^+CH_2(CH_2)_{11}CH_2\underline{CH_3}$}], 1.25–1.41 m [24H, {$N^+CH_2(\underline{CH_2})_{11}CH_2CH_3$ + $N(H)CH_2CH_2\underline{CH_2}CH_3$}], 1.47–1.54 m [2H, N(H)$CH_2\underline{CH_2}CH_2CH_3$], 1.73 s [2H, $N^+CH_2(CH_2)_{11}\underline{CH_2}CH_3$], 3.17 m (2H, N-$^+CH_2\underline{CH_2}OC$ = O), 3.47 s [6H, $N^+(\underline{CH_3})_2$], 3.61 s [2H, N(H)$\underline{CH_2}CH_2CH_2CH_3$], 3.95 s [2H, $N^+\underline{CH_2}(CH_2)_{11}CH_2CH_3$], 4.54 s (2H, N-$^+\underline{CH_2}CH_2OC$ = O), 6.07 bd.s [1H, N(H)$CH_2CH_2CH_2CH_3$]. ESI mass spectrum, *m*/*z*: 385.5 $[M\text{-}Br]^+$. Found, %:C 59.50; H 10.72; N 6.52; Br 16.58. $C_{23}H_{49}N_2O_2Br$. Calculated, %: C 59.33; H 10.61; N 6.02; Br 17.16. *M* 465.6.

N-[2-((butylcarbamoyl)oxy)ethyl]-*N*,*N*-dimethylhexadecaneammonium bromide (16Q^+-2-Ur-4) Yield 65%, mp 73–75 °C. IR spectrum, (KBr), *ν*, cm^{-1}: 3236, 2920, 2852, 1720, 1526, 1471, 1378, 1246, 1140, 1060, 969, 947, 721. ^{1}H NMR spectrum ($CDCl_3$, δ, ppm, *J*/Hz): 0.88–0.94 m [6H, {N(H)$CH_2CH_2CH_2\underline{CH_3}$ + $N^+CH_2(CH_2)_{13}CH_2\underline{CH_3}$}], 1.27–1.37 m [28H, {$N^+CH_2(\underline{CH_2})_{13}CH_2CH_3$ + $N(H)CH_2CH_2\underline{CH_2}CH_3$}], 1.51–1.54 m [2H, N(H)$CH_2\underline{CH_2}CH_2CH_3$], 1.75 s [2H, $N^+CH_2(CH_2)_{13}\underline{CH_2}CH_3$], 3.17 tr (2H, N-$^+CH_2\underline{CH_2}OC$ = O, *J* 6.67 Hz), 3.49 s [6H, $N^+(\underline{CH_3})_2$], 3.60 c [2H, N(H)$\underline{CH_2}CH_2CH_2CH_3$], 3.97 s [2H, $N^+\underline{CH_2}(CH_2)_{13}CH_2CH_3$], 4.56 s (2H, N-$^+\underline{CH_2}CH_2OC$ = O), 5.98 bd.s [1H, N(H)$CH_2CH_2CH_2CH_3$]; ESI mass spectrum, *m*/*z*: 413.5 $[M\text{-}Br]^+$. Found, %:C 60.50; H 10.14; N 5.28; Br 16.12. $C_{25}H_{53}N_2O_2Br$. Calculated, %: C 60.83; H 10.82; N 5.67; Br 16.19. *M* 493.6.

N-[2-((butylcarbamoyl)oxy)ethyl]-*N*,*N*-dimethyloctadecaneammonium bromide (16Q^+-2-Ur-4) Yield 79%, mp 70–72 °C. IR spectrum, (KBr), *ν*, cm^{-1}: 3236, 2919, 2851, 1720, 1526, 1401, 1375, 1247, 1140, 1060, 973, 947,853, 721. ^{1}H NMR spectrum ($CDCl_3$, δ, ppm, *J*/Hz): 0.86–0.94 m [6H, {N(H)$CH_2CH_2CH_2\underline{CH_3}$ + $N^+CH_2(CH_2)_{15}CH_2\underline{CH_3}$}], 1.25–1.37 m [32H, {$N^+CH_2(\underline{CH_2})_{15}CH_2CH_3$ + $N(H)CH_2CH_2\underline{CH_2}CH_3$}], 1.50–1.55 m [2H, N(H)$CH_2\underline{CH_2}CH_2CH_3$], 1.74 s [2H, $N^+CH_2(CH_2)_{15}\underline{CH_2}CH_3$], 3.13–3.18 m (2H, $N^+CH_2\underline{CH_2}OC$ = O), 3.48 c. [6H, $N^+(\underline{CH_3})_2$], 3.57–3.62 m [2H, N(H)$\underline{CH_2}CH_2CH_2CH_3$], 4.15 s [2H, $N^+\underline{CH_2}(CH_2)_{15}CH_2CH_3$], 4.54 s (2H, N-$^+\underline{CH_2}CH_2OC$ = O), 6.02 bd.s [1H, N(H)$CH_2CH_2CH_2CH_3$]. ESI mass spectrum, *m*/*z*: 441.6 $[M\text{-}Br]^+$. Found, %:C 62. 75; H 10.60; N 5.68; Br 14.98. $C_{27}H_{57}N_2O_2Br$. Calculated, %: C 62.19; H 11.02; N 5.37; Br 15.32. *M* 521.5.

N-[2-((ethylcarbamoyl)oxy)ethyl]-*N*,*N*-dimethylhexadecaneammonium bromide (16Q^+-2-Ur-2) Yield 78%, mp 75–76 °C. IR spectrum, (KBr), *ν*, cm^{-1}: 3231, 2923, 2852, 1718, 1541, 1468, 1377, 1263, 1158, 1068, 996, 905, 778, 722. ^{1}H NMR spectrum ($CDCl_3$, δ, ppm, *J*/Hz): 0.88 t [3H, $N^+CH_2(CH_2)_{13}CH_2\underline{CH_3}$, *J* = 6.9]; 1.19–1.15 t [3H, N(H)$CH_2\underline{CH_3}$, *J* = 7.2], 1.36–1.26 m [26H, $N^+CH_2(\underline{CH_2})_{13}CH_2CH_3$]; 1.74 [m, 2H, $N^+CH_2(CH_2)_{13}\underline{CH_2}CH_3$]; 3.25–3.18 m [2H, N(H)$\underline{CH_2}CH_3$]; 3.48 s [6H, $N^+(\underline{CH_3})_2$]; 3.62–3.58 m [2H, $N^+\underline{CH_2}(CH_2)_{13}CH_2CH_3$]; 3.97 s [2H, $N^+\underline{CH_2}CH_2OC$ = O]; 4.55 s [2H, N-$^+CH_2\underline{CH_2}OC$ = O]; 6.03 s [1H, N(H)$\underline{CH_2}CH_3$]; ESI mass spectrum, *m*/*z*:

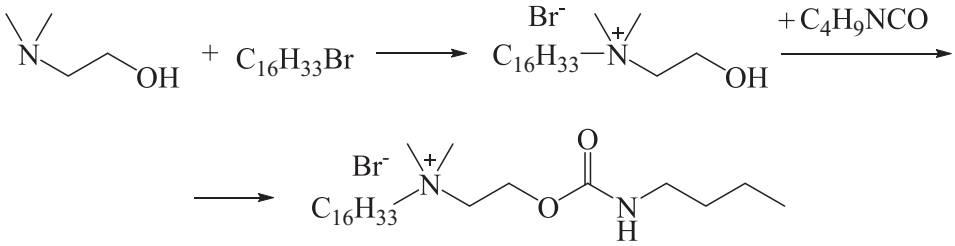

Scheme 1. The scheme of the synthesis of the carbamate-bearing surfactant **$16Q^+$-2-Ur-4**.

385.5 $[M\text{-}Br]^+$. Found, %:C 61.25; H 10.34; N 6.37; Br 16.52. $C_{23}H_{49}N_2O_2Br$. Calculated, %: C 60.33; H 10.61; N 6.02; Br 17.16. *M* 465.6.

N-[2-((butylcarbamoyl)oxy)propyl]-*N*,*N*-dimethylhexadecaneammonium bromide (16Q$^+$-3-Ur-4) Yield 72%, mp 120–122 °C. IR spectrum, (KBr), ν, cm^{-1}: 3231, 2923, 2852, 1718, 1541, 1468, 1377, 1263, 1158, 1068, 996, 905, 778, 722. ^{1}H NMR spectrum ($CDCl_3$, δ, ppm, *J*/Hz): 0.86–0.93 m [6H, {$N(H)CH_2CH_2CH_2\underline{CH_3}$ + $N^+CH_2(CH_2)_{13}CH_2\underline{CH_3}$}], 1.26–1.39 m [28H, {$N^+CH_2(\underline{CH_2})_{13}CH_2CH_3$ + $N(H)CH_2CH_2\underline{CH_2}CH_3$}], 1.48–1.55 m [2H, $N(H)CH_2\underline{CH_2}CH_2CH_3$], 1.73 s [2H, $N^+CH_2(CH_2)_{13}\underline{CH_2}CH_3$], 2.08 s (2H, $N^+CH_2\underline{CH_2}CH_2OC$ = O), 3.12–3.17 m (2H, $N^+CH_2CH_2\underline{CH_2}OC$ = O), 3.41–3.47 m {8H, [6H, $N^+(\underline{CH_3})_2$ + 2H, $N^+\underline{CH_2}CH_2CH_2OC$ = O]}, 3.89–3.93 m [2H, $N(H)\underline{CH_2}CH_2CH_2CH_3$], 4.16–4.18 m (2H, $N^+\underline{CH_2}CH_2CH_2OC$ = O), 6.07 bd.s [1H, $N(\underline{H})CH_2CH_2CH_2CH_3$]. ESI mass spectrum, *m*/*z*: 427.6 $[M\text{-}Br]^+$. Found, %: C 62.12; H 10.60; N 5.86; Br 15.42. $C_{23}H_{49}N_2O_2Br$. Calculated, %: C 61.51; H 10.92; N 5.52; Br 15.74. *M* 507.6.

2.3. Instruments and methods

Surface tension measurements were performed by the anchor-ring method using KRUSS 6 tensiometer. The cmc values were defined as the concentration corresponding to the breakpoints in the γ vs. logarithm of surfactant concentration plots. The surface excess Γ_{max} and the surface area per a molecule, A_{min}, have been calculated using the Gibbs equation: $\Gamma_{max} = \frac{1}{2.3nRT}\lim_{C\to cmc}(d\pi/d\log C)$, were R = 8.31 J mol K^{-1} (gas constant), π is the surface pressure obtained from the surface tension of water minus the surface tension of the surfactant solution, and *T* is the absolute temperature in K. N_A is Avogadro number (6.02×10^{23} mol^{-1}). The parameter *n* represents the number of species at the interface the concentration of which changes with surfactant concentration. The constant *n* takes the value 2 for an ionic surfactant where the surfactant ion and the counterion are univalent; $A_{min} = 10^{18} / (N_A \times \Gamma_{max})$.

Specific conductivities were measured with Inolab Cond 720 conductometer. Krafft points were determined in the 1% surfactant solutions. The solution was cooled to precipitation of the surfactant and then, as the solution was exposed to heating at a rate of 0.5 °C/min, conductivities of the supernatant fluid were measured.

Solubilization effects toward the Orange OT in the micellar systems were determined as described elsewhere [27] by following the change in the absorbance of their saturated solutions with concentration of the surfactant added. The spectra were recorded in the range from 250 to 600 nm with Specord-250 Plus spectrophotometer using the thermostated quartz cells of a 0.5–1.0 cm path length.

Fluorescent spectra of pyrene at a concentration of $1 \cdot 10^{-6}$ $mol \cdot L^{-1}$ in the solutions of the surfactants were recorded using Varian Cary Eclipse spectrophotometer. Emission spectra were recorded within the interval of 350–500 nm at a scanning rate of 120 nm/min using a 1.0 cm path length cuvette; the excitation of the sample was occurred at a wavelength of 335 nm.

The following microorganisms were used when studying the antimicrobial activity: *Staphylococcus aureus ATCC 209p*, *Escherichia coli CDC F 50*, *Bacillus cereus ATCC 8035*, *Trichophyton mentagrophytes* var. *gypseum 1773*, *and Candida albicans VKPGu401/NCTC885 653*. The bacteriostatic properties were studied by serial dilutions [28]. The bacterial load in the experimental run was 300,000 microbial cells per 1 mL (cells/mL). The fungistatic activity of the compounds was studied by serial dilutions on Saburo medium according to procedure [29].

Investigation of acute toxicity was carried out according to [30]. Each dose was administered intraperitoneally to five mice (22–24 g in mass). As a value of toxicity, LD_{50} was used, which was calculated graphically according to Behrens (original program, Arbuzov Institute of Organic and Physical Chemistry, R "version 2.13.0" (2011–04-13)). All experiments involving animals were performed in accordance with the guidelines set forth by the European Communities Council Directive of November 24, 1986 (86/609/EEC) and the protocol of experiments approved by the Animal Care and Use Committee of Kazan State Medical University.

DPPC liposomes for turbidimetric measurements were prepared as follows: 5.4 mg of DPPC was dissolved in 60 μL $CHCl_3$ and kept overnight at room temperature for solvent evaporation. Obtained lipid thin film was suspended in water at 60 °C and vigorous stirring. After that dispersion was heat treated: alternately cooled down in liquid nitrogen and heated at water bath at 60 °C. This procedure was repeated three times. Suspension was extruded through LiposoFast Basic ("Avestin") extruder using carbohydrate filter with 100 nm pore diameter. Prepared liposomes were diluted to 0.7 mM and used in turbidimetric measurements at Specord 250 PLUS ("Analytik Jena") spectrophotometer. Primary turbidimetric plots were treated in terms of Van't Hoff two-state model. In accordance with this approach break point in the plot corresponds to the main phase transition of DPPC from gel to liquid crystalline phase [31].

3. Results and discussion

3.1. Aggregation behavior of carbamate-bearing surfactants in aqueous solutions. Tensiometry and conductometry studies

Surface tension isotherms, which are recorded using tensiometry method, primarily provide the determination of the concentration ranges of micelle formation of the compounds under study. Derived from the dependences given in Fig. 1, critical micelle concentrations were determined in the case of the carbamate-bearing surfactants.

As follows from the data (Table 1), the cmc value of these compounds is significantly less than that of their unsubstituted trimethylammonium counterparts (see, for example, **16Q$^+$-2-Ur-4** and CTAB). It can be considered that the ability of urethane compounds to form hydrogen bonds [25,32] facilitates self-organization of these compounds in solution. There is a linear relationship between the logarithm of cmc of surfactants and the number of carbon atoms (n) in hydrophobic tail, which is described for the surfactants under study as follows: lg (cmc) = 0.563–0.257 × n, (R = 0.997). The values of the free component (A = 0.563) and angular coefficient (B = 0.257) of the above linear plot for carbamate-bearing surfactants are slightly different from those of ionic surfactants (usually A = 1.5–1.9 and B = 0.3) [33]. The presence of carbamate fragment in the head group of

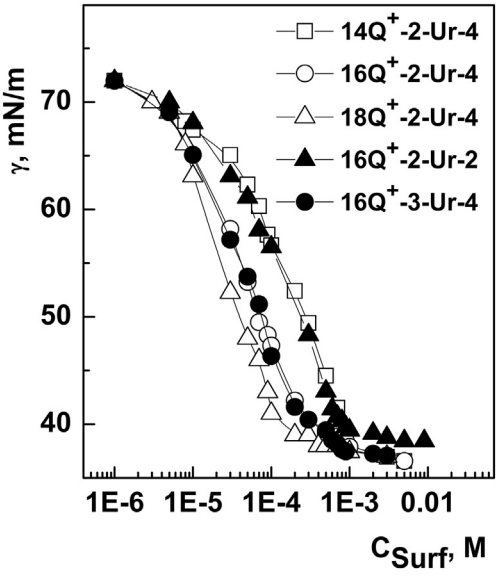

Fig. 1. Surface tension isotherms of the carbamate-bearing surfactants: (25 °C).

Table 1
The values of maximum adsorption (Γ_{max}), the minimum surface on one surfactant molecule (A_{min}), free energy of micelle formation (ΔG_m), and the standard free energy of adsorption (ΔG_{ad}) of aqueous solutions of carbamate-bearing surfactants.

Surfactant	cmc, mM	A_{min} nm^2	Γ_{max} 10^6 mol·m^{-2}	ΔG_m kJ·mol^{-1}	ΔG_{ad} kJ·mol^{-1}	γ_{cmc} mN·m^{-1}
14Q$^+$-2-Ur-4	1.0	1.74	0.96	−26.1	−58.0	41.5
16Q$^+$-2-Ur-4	0.24	1.36	1.22	−32.2	−56.8	42.0
18Q$^+$-2-Ur-4	0.09	0.98	1.69	−35.2	−54.7	41.0
16Q$^+$-2-Ur-2	0.70	1.63	1.02	−27.5	−58.2	40.7
16Q$^+$-3-Ur-4	0.28	1.22	1.36	−29.2	−53.1	39.5

surfactant, which is capable of hydrogen bonding, presumably contributes to the interactions with water dipoles as compared to trimethylammonium counterparts, which is reflected in aggregation characteristics. It should be emphasized that hydrophobic effect mainly contributes to the aggregation of amphiphilic compounds in aqueous solutions. At the same time additional factors can be responsible for the self-assembling of amphiphiles. In particular, hydrogen bonding provides multicentered interactions of surfactant molecules around them and with water, thereby promoting pre-organization of surfactant molecules below the cmc, decreasing the electrostatic repulsion of head groups, and favoring their hydration. Usually, such functionalized surfactants are characterized by lower cmc values, compared to their trimethylammonium analogs [34–36].

Derived from tensiometry data (Fig. 1), adsorption parameters of the systems were calculated. The results are given in Table 1. As in the case of most surfactants, adsorption and micelle formation of the carbamate-bearing surfactants are thermodynamically favorable processes and occur spontaneously in aqueous solutions (free adsorption and micelle formation energies become negative). With elongation of the surfactant's hydrophobic tail, these processes are facilitated, which is reflected in the growth of the absolute value of ΔG_m, ΔG_{ad} and the values of maximum adsorption. In parallel, the area occupied by a surfactant molecule in the adsorption layer decreases, which probably reflects its denser packing. This is influenced by both the structure of head group and alkyl tail length. In particular, an increase in the conformational lability of hydrocarbon tail can control the steric approach of surfactant molecules upon their adsorption at the interface. Similar trend in the variation of adsorption parameters is typical for homological series of cationic surfactants with trimethylammonium group [37], as well as for cationic surfactants with a bulkier head group [38].

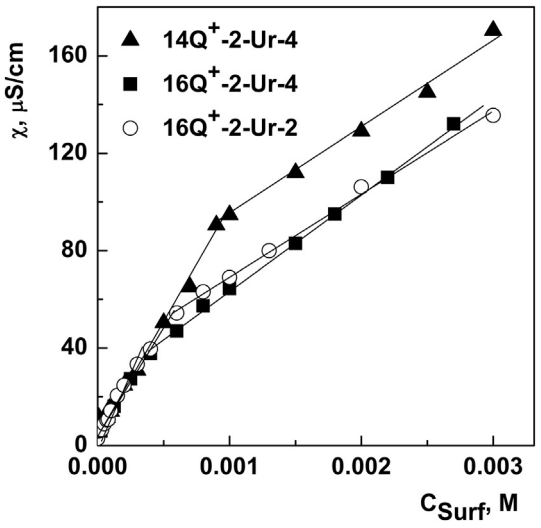

Fig. 2. The dependence of the specific electroconductivity of the carbamate-bearing surfactants on the concentration (25 °C).

Table 2
The values of cmc, degree of counterion binding (β), and Krafft point of the carbamate-bearing surfactants determined by conductometry (1 wt%).

Surfactant	cmc, mM	β	T_{Kr}, °C
14Q$^+$-2-Ur-4	0.98·	0.56	13
16Q$^+$-2-Ur-4	0.32	0.51[a]	10
18Q$^+$-2-Ur-4	0.13	0.55	19[b]
16Q$^+$-2-Ur-2	0.62	0.54	15
16Q$^+$-3-Ur-4	0.70	0.46	11

[a] In the case of CTAB β is 0.74.
[b] 1 wt% solution is very viscous, which is inconvenient for work and decreases the correctness of measurements, so the sample was tested at the surfactant concentration of 0.5 wt%.

The influence of the temperature on cmc is exemplified by **16Q$^+$-2-Ur-4**. An increase in the temperature within the range from 25 to 37 °C is accompanied by a slight increase in cmc values from 0.24 to 0.29 mM. Surface tension isotherms for this surfactant and their quantitative treatment in terms of Gibbs equation are given in Supporting Information section (Fig.S1 and Table S1).

Tensiometry data are strongly supported by conductometry studies. For example, the cmc values determined from concentration dependences of the specific electroconductivity of carbamate-bearing surfactants (Fig. 2 and Table 2), agree well with the values given in Table 1, which emphasizes the reliability of the results. In addition, the degree of counterion binding with micelles was calculated from the dependences: $\beta = 1\text{-}\alpha$, where α is the degree of dissociation, defined as the ratio of slopes of the sections of the dependence before and after cmc (Table 2).

The values of β of a series of carbamate-bearing surfactants under study differ insignificantly; however, they are remarkably less than those of analogous trialkylammonium surfactants (note to Table 2). Similar behavior is observed for cationic surfactants bearing bulky moieties in head groups, preventing their binding with counter-ions [39,40]. This suggests that counterions of the surfactants under study compensate for the charge of carbamate-bearing head groups to the lower extent, which should be reflected in lower aggregation numbers.

On the contrary, one can determine the critical micelle temperature from the temperature dependences of electroconductivity (Figs. 3, S2), which is characterized by the Krafft point (T_{Kr}). The values of T_{Kr} of the carbamate-bearing surfactants are in the range below 15 °C (Table 2), which is significantly less than those of their unsubstituted trimethylammonium counterparts. Thus, the essential benefit of surfactants under study is that the concentration and temperature thresholds of their micelle formation are lower than those of conventional cationic surfactants.

3.2. Solubilizing effect of the carbamate-bearing surfactants with respect to hydrophobic probes (Orange OT and pyrene)

An important feature of micelles, which determines their practical application, is their ability to solubilize hydrophobic compounds. In this work, the solubilization of low-polar dyes represented by Orange OT was studied.

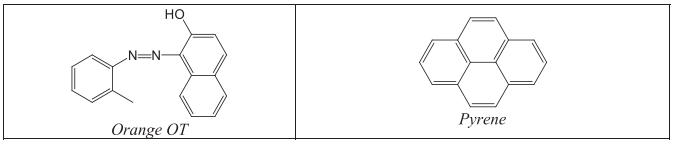

This dye characterized by the intense absorption band in the range of 490–500 nm, is widely used as a high-sensitive probe for the quantitative evaluation of the solubilization capacity of the systems based on surfactants [41]. The comparison of the literature data and the results of the compounds with carbamate fragments gives an estimate of

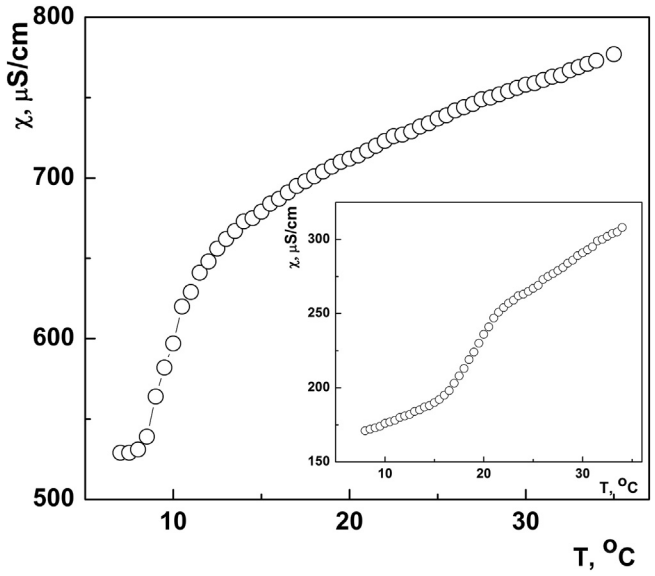

Fig. 3. The dependence of the specific electroconductivity of the carbamate-bearing surfactant **16Q$^+$-2-Ur-4** on temperature (1 wt%). On the inset: The dependence of the specific electroconductivity of the surfactant **18Q$^+$-2-Ur-4** on temperature (0.5 wt%).

their effectiveness among known surfactants. In Figs. 4 and 5, spectrophotometric data on the solubility of Orange OT depending on the concentration of surfactant are given.

The initial section of the dependence (Fig. S3) reflects the fact that Orange OT almost does not dissolve in water. The appearance of micelles, capable of solubilizing the dye and thus increase its content in solution, is accompanied by the drastic increase in absorbance. The break point on these dependences corresponds to cmc. The determined values (Table 3) agree well with the results, which were determined from tensiometry and conductometry (Tables 1 and 2). In addition, the solubilization capacity of micelles (S) can be derived from the dependences given in Figs. 5 and S3. $S = b/\varepsilon$, where b is the slope of $D/L = f(C)$, ε is the absorption coefficient, D is the absorbance at 495 nm, L is the cell thickness, and C is the concentration of surfactant. As follows from the results (Table 3), the solubilization capacity of the surfactants depends primarily on the alkyl chain length and it increases with a transition from tetradecyl to octadecyl derivative. The presence of carbamate fragment also favors the solubilization of hydrophobic probes: as can be seen from S values (Table 3), hexadecyl derivatives (**16Q$^+$-2-Ur-4**, **16Q$^+$-2-Ur-2, 16Q$^+$-3-Ur-4**) are nearly two times as effective as their CTAB counterpart. Probably the existence of the fragment capable of

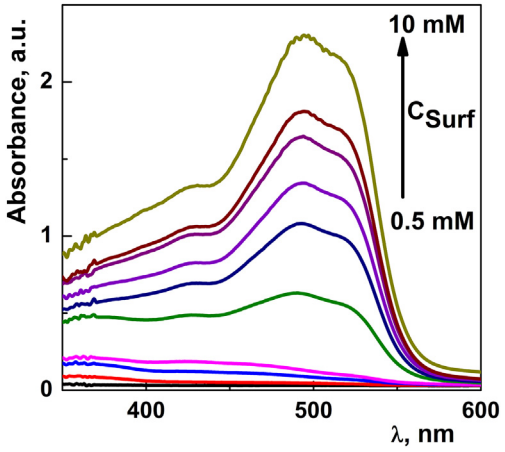

Fig. 4. Spectra of saturated solutions of Orange OT recorded at various surfactant concentrations.

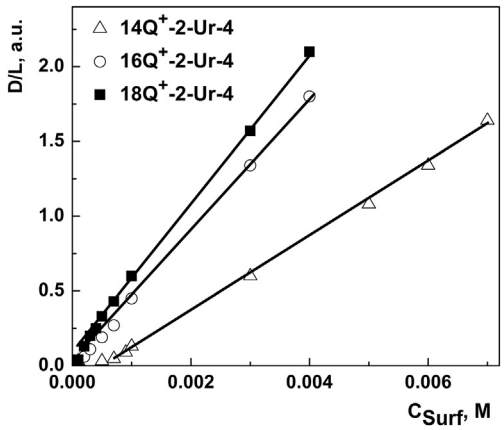

Fig. 5. Changes of the absorbance of saturated solutions of Orange OT at the wavelength of 500 nm depending on the surfactant concentration.

hydrogen bonding, involves additional mechanisms of the interaction between dye and micelle, which facilitates solubilization processes.

Valuable information can be obtained from the data analysis of the solubilization of Orange OT using Schott approach [42], which evaluates the molecular mass of micelle (MMm), as well as aggregation numbers (n). This approach is based on the assumption that dye does not dissolved below cmc, while only one of its molecules solubilize in micelle above cmc. In spite of the fact that Schott approach is not highly precise (primarily due to the fact that the equivalent dye-to micelle ratio is not always fulfilled), its use is valid when comparing aggregation numbers of surfactants of one series. In addition, there are many examples of the agreement of the data on the solubilization of Orange OT with neutron scattering or dynamic light scattering [27,43].

The results, which were obtained by us using Schott method in the case of carbamate-bearing surfactants, are given in Table 3. They state that, with an increase in the hydrocarbon chain length, there is a decrease in the aggregation number, while the change of the structure of head group has a smaller effect. However, aggregation numbers of carbamate-bearing surfactants are less than those of their trialkylammonium counterparts (note to Table 3). The lower charge compensation, observed in the case carbamate-bearing head groups (see binding values of counterions in Table 2), presumably prevents aggregation of a larger number of molecules. With the growth of the concentration of surfactant in solution, the value of n slightly increases; however, its drastic increase occurs only at the concentrations, which exceed the cmc value by the factor of 10–20. This is presumably related to the violation of the spherical shape of micellar aggregates.

Pyrene was one more hydrophobic compound, which was used to characterize surfactant. This compound is widely employed in research as a sensitive fluorescent probe [45–47]. The position of emission maxima of this compound depends little on solvent, while their intensity is sensitive to the change of environmental factors, in particular, the polarity of microenvironment. We recorded fluorescence spectra of pyrene in

Table 3
Solubilization[a] capacity, critical micelle concentration, molecular mass of micelles, and aggregation numbers, which were determined using Orange OT dye.

Surfactant	cmc, mM	S	MMm	n	MMm	n
			at C/cmc = 3		at C/cmc = 5	
14Q$^+$-2-Ur-4	1.2	0.012	29,124	62	32,309	69
16Q$^+$-2-Ur-4[b]	0.21	0.024	16,224	32	17,745	35
18Q$^+$-2-Ur-4	0.1	0.207	10,202	20	12,130	23
16Q$^+$-2-Ur-2	0.75	0.027	15,687	29	13,719	34
16Q$^+$-3-Ur-4	0.25	0.022	19,013	37	20,363	40

[a] Solubilization capacity is the number of moles of dye on one mole of surfactant.
[b] In the case of CTAB, the solubilization capacity of Orange OT is 0.015 [41] and aggregation numbers at the concentration, which is five times as high as cmc, are 66.8 [44].

the solutions of carbamate-bearing surfactants at their various concentrations. A typical form of the spectra is given in Fig. 6. The parameter, which evaluates the effect of medium, is the intensity ratio of the first peak at 373 nm (I_I) to the third peak at 384 nm (I_{III}) [48]. This ratio (I_I/I_{III}) is sensitive to micropolarity in the localization area of probe and usually decreases with an increase in the concentration of surfactant, because there is a decrease in the polarity of microenvironment.

Results of the analysis of emission spectra of pyrene in the solutions of carbamate-bearing surfactants and the change of the ratio (I_I/I_{III}) depending on the content of surfactant are given in Fig. 7. The dependences are characterized by two sections with different slopes, whose intersection point corresponds to cmc. The cmc values, which were obtained using fluorescence method, coincide well with the data of other methods (Table S2).

Derived from the I_I/I_{III} peak ratio, the polarity of the head group of surfactant and the localization of pyrene in micelles can be stated. In the case of pyrene dissolved in water, the value of I_I/I_{III} is 1.51. If I_I/I_{III} < 0.6, the probe is located in the hydrocarbon core of the micelle. The location of pyrene in the surface layer of micelles is characterized by the ratio of 1.0–1.4. In the case of the carbamate-bearing surfactants under study, the value of I_I/I_{III} varies in the range of 1.01–1.08 (Fig. 7). This indicates that pyrene is localized in the surface layer of micelles. The highest value of I_I/I_{III} is related to compound **16Q$^+$-2-Ur-2**. The presence of ethyl substituent in the head group of this compound presumably provides the penetration of a larger quantity of water inside the micelle than in the case of more hydrophobic butyl fragment. In addition, there is a decrease in micropolarity in the following order: **16Q$^+$-2-Ur-4** < **16Q$^+$-2-Ur-4** < **16Q$^+$-2-Ur-4**.

Excimer fluorescence of pyrene should be noted, which manifests itself in the solutions of carbamate-bearing surfactants, which appears in the form of broad band with the maximum of nearly 470 nm in spectra (Fig. 6). This phenomenon usually arises, when pyrene molecules can arrange in a stacking manner, and occurs at its high concentration in solution or micellar phase [49,50]. The presence of excimer fluorescence indicates a high solubilizing effect of the surfactants. Maximum intensities of this band are achieved in the c case of surfactant **18Q$^+$-2-Ur-4**, which agrees with the data on its highest solubilization capacity in a series of the compounds.

3.3. Toxicity and antimicrobial effect of carbamate-bearing surfactants

One of the requirements to surfactants during their practical application, in particular, in the fields, which are related to their contact with living organisms, is low toxicity. Most cationic surfactants do not fulfill

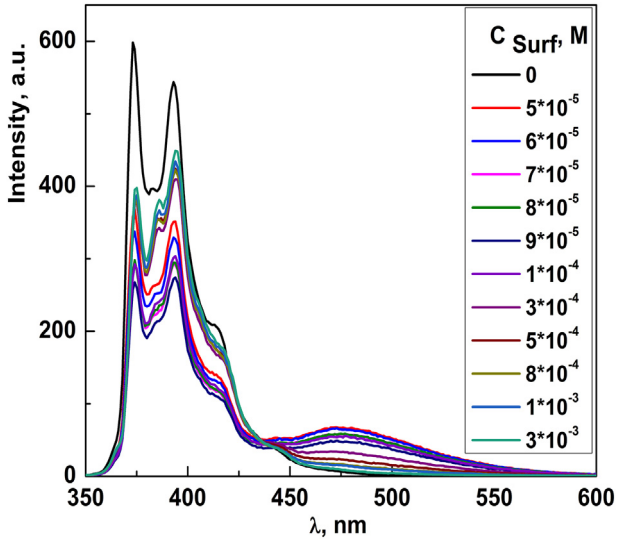

Fig. 6. Fluorescence spectra of pyrene in the case of the surfactant **18Q$^+$-2-Ur-4**.

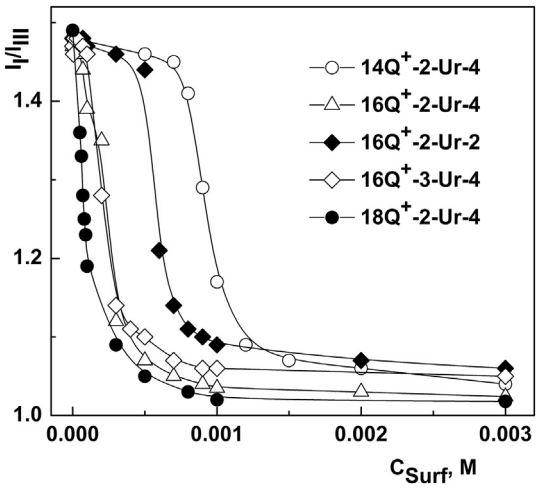

Fig. 7. Variation of the I_I/I_{III} ratio depending on concentration of carbamate-bearing surfactants.

these requirements in spite of broad possibilities of their practical application. One example is that conventional reference surfactant, such as CTAB, possesses LD_{50} of 27 mg/kg (mice, intraperitoneal administration) and is related to 4 class of danger [51]. The values of LD_{50} of carbamate-bearing surfactants at the same way of administration of substance are in the range of 80–100 mg/kg (note to Table 4); i.e., they are related to the class of moderately toxic surfactants. This fact, as well as low aggregation threshold of the compounds, which provides a decrease in working concentrations of substance along with its high effect, indicate practical potential of carbamate-bearing surfactants.

At the final stage of the work we tested the antimicrobial activity of the surfactants. The following microorganisms were used as test objects: Gram-positive bacteria *Staphylococcus aureus ATCC 209p* (*Sa*), *Bacillus cereus ATCC 8035* (*Bc*), a Gram-negative bacteria *Escherichia coli CDC F-50* (*Ec*) *and a fungi*, *Trichophytonmentagrophytes* var. *gypseum 1773* (*Tm*), *Candida albicans VKPGu401/NCTC 885–653* (*Ca*). As follows from the results in Table 4 the synthesized series of carbamate-bearing surfactants exhibits both antibacterial and antifungal activity. Among the samples studied the highest effect occurs for the compounds 1a and 1b. Besides, specificity of the action is observed: e.g. efficacy of 1a against *Staphylococcus aureus* и *Escherichia coli* is higher compared to compound 1a, while in the case of *Trichophyton mentagrophytes* the

Table 4
Antibacterial and antifungal properties of the carbamate-bearing surfactants[a].

Specimen	*Sa*	*Bc*	*Ec*	*Tm*	*Ca*
Minimum inhibition concentration, μg/mL[b]					
14Q$^+$-2-Ur-4	0.5 ± 0.04	1.9 ± 0.2	7.8 ± 0.5	15.6 ± 1.2	1.9 ± 0.1
16Q$^+$-2-Ur-4	1.9 ± 0.1	1.9 ± 0.2	62.5 ± 5.8	7.8 ± 0.6	3.9 ± 0.2
18Q$^+$-2-Ur-4	3.9 ± 0.3	7.8 ± 0.5	125 ± 11	15.6 ± 1.4	7.8 ± 0.5
16Q$^+$-2-Ur-2	1.9 ± 0.2	1.9 ± 0.1	15.6 ± 1.2	15.6 ± 1.3	7.8 ± 0.4
Norfloxacin	2.4 ± 0.2	7.8 ± 0.6	1.5 ± 0.1		
Ketoconazole				4.0 ± 0.3	4.0 ± 0.2
CTAB [51]	0.5	3.1	6.3	31.3	3.1
Minimal concentrations inducing the cell death, μg/mL[b]					
14Q$^+$-2-Ur-4	7.8 ± 0.6	31.3 ± 2.5	7.8 ± 0.6	31.3 ± 2.8	7.8 ± 0.7
16Q$^+$-2-Ur-4	3.9 ± 0.3	62.5 ± 5.7	250 ± 22	125 ± 12	3.9 ± 0.1
18Q$^+$-2-Ur-4	31.3 ± 2.6	125 ± 10	—	62.5 ± 5.9	7.8 ± 0.7
16Q$^+$-2-Ur-2	3.9 ± 0.2	62.5 ± 5.4	15.6 ± 1.3	15.6 ± 1.4	7.8 ± 0.5
Norfloxacin	2.4 ± 0.2	15.6 ± 1.2	1.5 ± 0.1		
Ketoconazole				4.0 ± 0.3	4.0 ± 0.2
CTAB [51]	50	>500	>500	500	50

[a] LD_{50} (mice, intraperitoneal administration), mg/kg is: 95 (**14Q$^+$-2-Ur-4**), 82 (**16Q$^+$-2-Ur-4**), 93 (**18Q$^+$-2-Ur-4**), 92(**16Q$^+$-2-Ur-2**), 78 (**16Q$^+$-3-Ur-4**).
[b] The tests were performed in duplicate and repeated twice; (—) MIC >500 μg.mL^{-1}.

revers effect is observed. The comparison of antimicrobial activity 1a and 1b and their nonfunctionalized analog, CTAB makes it possible to conclude that the introduction of carbamate moiety improves fungistatic properties. Besides, in the case of the surfactants under study bactericidal activity and fungicidity appeared which is nontypical for cationic surfactants. Parallel comparison of the activity of compounds 1a and 1b with that of commercial antibacterial preparation Norfloxacin and antifungal agent Ketoconazole revealed the close effect. Moreover, the activity of carbamate-bearing surfactants against *Staphylococcus aureus* и *Candida* is even higher than in the case of reference compounds. Noteworthy, the undoubted advantage of carbamate-bearing surfactants is the possibility of manifestations of both antibacterial and antifungal properties.

The results agree with recent considerations on the mechanism of antimicrobial action of cationic surfactants, which suggests their adsorption on the outer cellular membrane of the microorganism due to their amphipathic characteristics. As a result of the adsorption, surfactant molecules penetrate through the cell membrane; furthermore the positively charged molecules neutralize the negative charges on the bacterial cell membranes. Accordingly, the selective permeability which characterizes the outer cellular membrane is completely deactivated. Hence, the vital transportation of essential components, bio-reactions and activities of the cell are disturbed, causing death for these microorganisms. The structure of surfactants markedly influences their adsorption and penetration characteristics. Typically, the antimicrobial versus surfactant concentration dependences have the extremum type, with maximum effect observed for tetradecyl and hexadecyl derivatives. The maximum effect can be shifted depending on the microorganism type and the nature of head group [38,52].

The ability of carbamate-bearing surfactants to integrate into lipid bilayers was confirmed by us on the example of **16Q$^+$-2-Ur-4**. As a simplest model of biomembranes, liposomes based on dipalmitoylphosphatidylcholine were used. The crucial characteristic of a lipid bilayer is the temperature of the main phase transition which can be affected by the intercalation of foreign substances, e.g. surfactants [53,54]. When the amount of **16Q$^+$-2-Ur-4** was varied, phase transition of membranes from the liquid-crystalline to more ordered gel state was studied using turbidimetry. Typical turbidimetric dependences, which were obtained during experiment (Fig. S4), were mathematically treated within the model of two states [31].

The results of treatment were visualized in Fig. 8 in the form of the dependence of the temperature of main phase transition (T_{PT}) of the lipid on the molar ratio of components in the case of the surfactant–DPPC system.

The addition of the surfactant **16Q$^+$-2-Ur-4** leads to a small linear decrease in temperature until the surfactant-to-lipid ratio of 0.1,

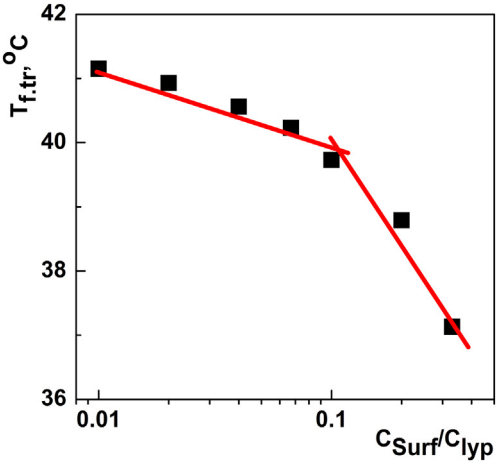

Fig. 8. Dependence of the temperature of main phase transition of DPPC on the surfactant-to-DPPC molar ratio.

which confirms the incorporation of the surfactant into liposome. There is a drastic decrease of the temperature of main phase transition above this value, which indicates the solubilization of membrane with micelles. The result confirms the possibility of the violation of the integrity of lipid membrane with the introduction of surfactant, which may lead to the death of microbial cell.

4. Conclusions

In this work, novel carbamate-bearing cationic surfactants have been designed to fabricate biodegradable nanocontainers for hydrophobic guests. Their aggregation in bulk phase and adsorption at the interface are examined by different techniques. The role of surfactant structure in the self-assembling behavior was discussed from the viewpoint of the ability of hydrogen bonding. Solubilization of hydrophobic dyes (Orange OT and pyrene) has been employed to determine aggregation numbers, evaluate solubilization capacity of micelles, and characterize micropolarity in the localization area of probe. It has been shown that the surfactants can be related to the class of moderately toxic compounds. Investigation of antimicrobial properties of carbamate-bearing surfactants has demonstrated their significant antibacterial and antifungal activity. Importantly, these surfactants have a pronounced ability to integrate with lipid bilayer. Based on the data obtained supramolecular systems composed of the carbamate-bearing surfactants can be recommended as helpful biodegradable nanocontainers capable of effective binding the hydrophobic active molecules and allowing them to pass through biological barriers.

Acknowledgement

AM, LZ and OS thank Russian Science Foundation; grant No. 14-23-00073 (the study of solubilization of hydrophobic probes).

Appendix A. Supplementary data

Supplementary data to this article can be found online at https://doi.org/10.1016/j.molliq.2018.08.007.

References

[1] Th.F. Tadros, Applied Surfactants: Principles and Application, Wiley-VCH, Weinheim Germany, 2005.
[2] S. Matile, A.V. Jentzsch, J. Montenegro, A. Fin, Recent synthetic transport systems, Chem. Soc. Rev. 40 (2011) 2453–2474.
[3] L.Ya. Zakharova, A.B. Mirgorodskaya, E.P. Zhiltsova, L.A. Kudryavtseva, A.I. Konovalov, Reactions in supramolecular systems, in: U.H. Brinker, J.-L. Mieusset (Eds.), Molecular Encapsulation: Organic Reactions in Constrained Systems, John Willey and Sons, Chichester, U.K. 2010, pp. 397–420.
[4] F. Devínsky, M. Pisárčik, M. Lukáč, Cationic Amphiphiles: Self-assembling Systems for Biomedicine and Biopharmacy, Nova Science Publishers, Inc., 2017
[5] R. Zana, J. Xia, Gemini Surfactants: Synthesis, Interfacial and Solution-phase Behavior, and Applications, New York, 2004.
[6] R. Sharma, A. Kamal, M. Abdinejad, R.K. Mahajan, H.-B. Kraatz, Advances in the synthesis, molecular architectures and potential applications of gemini surfactants, Adv. Colloid Interf. Sci. 248 (2017) 35–68.
[7] A.B. Mirgorodskaya, L. Ya Zakharova, E.I. Khairutdinova, S.S. Lukashenko, O.G. Sinyashin, Supramolecular systems based on gemini surfactants for enhancing solubility of spectral probes and drugs in aqueous solution, Colloids Surf. A Physicochem. Eng. Asp. 510 (2016) 33–42.
[8] M. Waligórska, A. Szulc, B.J. Brycki, The biodegradation of monomeric and dimeric alkylammonium surfactants, Hazard. Mater. 280 (2014) 797–815.
[9] A. Tehrani-Bagha, K. Holmberg, Cleavable surfactants, Curr. Opin. Colloid Interface Sci. 12 (2007) 81–91.
[10] D. Xu, X. Ni, C. Zhang, J. Mao, Ch. Song, Synthesis and properties of biodegradable cationic gemini surfactants with diester and flexible spacers, J. Mol. Liq. 240 (2017) 542–548.
[11] M.C. Moran, A. Pinazo, L. Perez, P. Clapes, M. Angelet, M.T. Garcia, M.P. Vinardell, M.R. Infante, Green amino acid-based surfactants, Green Chem. 6 (2004) 233–240.
[12] D.R. Gabdrakhmanov, D.A. Samarkina, V.E. Semenov, E.S. Krylova, V.S. Reznik, L.Ya. Zakharova, Cationic surfactant with 1,2,4-triazole- and uracil moieties as amphiphilic building blocks for supramolecular nanocontainers, J. Mol. Liq. 21 (2016) 255–259.
[13] D.R. Gabdrakhmanov, F.G. Valeeva, V.V. Syakaev, S.S. Lukashenko, S.K. Latypov, L.Ya. Zakharova, O.G. Sinyashin, S.V. Zakharov, D.A. Kuryashov, N.Y. Bashkirtseva, Novel

supramolecular system based on a cationic amphiphile bearing glucamine fragment: structural behavior and hydrophobic probe binding, Mendeleev Commun. 25 (2013) 174–176.
[14] A. Pinazo, M.A. Manresa, A.M. Marques, M. Bustelo, M.J. Espuny, L. Pérez, Amino acid–based surfactants: new antimicrobial agents, Adv. Colloid Interf. Sci. 228 (2016) 17–39.
[15] C. Gamerith, E.H. Acero, A. Pellis, A. Ortner, R. Vielnascher, D. Luschnig, B. Zartl, K. Haernvall, S. Zitzenbacher, G. Strohmeier, O. Hoff, G. Steinkellner, K. Gruber, D. Ribitsch, G.M. Guebitz, Improving enzymatic polyurethane hydrolysis by tuning enzyme sorption, Polym. Degrad. Stab. 132 (2016) 69–77.
[16] B.R. Mohapatra, Biocatalytic efficacy of immobilized cells of *Chryseobacterium* sp. Alg-SU10 for simultaneous hydrolysis of urethane and urea, Biocatal. Biotransform. (2018) 1–9.
[17] M. Ramirez-Huerta, I.J. Zvonkina, M.D. Soucek, Phenyl carbamate end-capped oligoesters: a model for hydrolytic stability of ester-based urethanes, J. Coat. Technol. Res. 13 (2016) 781–793.
[18] M. Mehta, A. Adem, M. Sabbagh, New acetylcholinesterase inhibitors for Alzheimer's disease, Int. J. Alzheimers Dis. 2012 (2012) 728–983.
[19] C. Holmes, D. Wilkinson, Molecular biology of Alzheimer's disease, Adv. Psychiatr. Treat. 6 (2000) 193–200.
[20] S.K. Tippabhotla, N.R. Thudi, R. Raghuvanshi, A.H. Khuroo, S. Gurule, S. Mishra, T. Monif, V.K. Lao, A bioequivalence study comparing two formulations of lopinavir/ritonavir capsules, Int. J. Clin. Pharmacol. Ther. 46 (2008) 204–210.
[21] X. Wang, H. Mu, H. Chai, D. Liao, Q. Yao, C. Chen, Human immunodeficiency virus protease inhibitor ritonavir inhibits cholesterol efflux from human macrophage-derived foam cells, Am. J. Pathol. 171 (2007) 304–314.
[22] G. Indolfi, D. Serranti, M. Resti, Direct-acting antivirals for children and adolescents with chronic hepatitis C, Lancet Child Adolesc. Health 2 (4) (2018) 298–304.
[23] C. Sikavi, H.Ph. Chen, A.D. Lee, E.G. Saab, G. Choi, S. Saab, Hepatitis C and human immunodeficiency virus coinfection in the era of direct-acting antiviral agents: no longer a difficult-to-treat population, Hepatology 67 (2018) 847–857.
[24] V.Y. Goloborodko, M.V. Strelkov, A.A. Kalinin, V.A. Byvaltsev, Analysis of efficacy of using nondepolarizing muscle relaxant rocuronium bromide and selective antidote sugammadex while providing general anesthesia to patients with degenerative spinal canal stenosis of the cervical spine, New Armenian Medical J. 11 (2017) 70–75.
[25] S.A. Rizvi, L. Shi, D. Lundberg, F.M. Menger, Unusual aqueous-phase behavior of cationic amphiphiles with hydrogen-bonding headgroups, Langmuir 24 (3) (2008) 673–677.
[26] A. Chatterjee, C.S. Maiti, S.K. Sanyal, S.P. Moulik, D. Das, P. Das, Langmuir, 18, 2002 2998–3004Langmuir19, 2002 9114–9119.
[27] A.B. Mirgorodskaya, E.I. Yackevich, F.G. Valeeva, V.A. Pankratov, L.Ya. Zakharova, Solubilizing and catalytic properties of supramolecular systems based on gemini surfactants, Russ. Chem. Bull. 63 (2014) 82–87.
[28] E.A. Ved'mina, N.M. Furer, Encyclopedic Handbook on Microbiology, Clinical Aspects, and Epidemiology of Infectious Diseases, Meditsina, Moscow, 1964.
[29] S.E. Milovanova, Methods of Experimental Chemotherapy, Meditsina, Moscow, 1971.
[30] I.V. Berezovskaya, Classification of substances with respect to acute toxicity for parenteral administration, Pharm. Chem. J. 37 (2003) 139–142.
[31] H.M. Seeger, G. Marino, A. Alessandrini, P. Facci, Effect of physical parameters on the main phase transition of supported lipid bilayers, Biophys. J. 97 (2009) 1067–1076.
[32] A. Bertrand, F. Lortie, J. Bernard, Routes to hydrogen bonding chain-end functionalized polymers, Macromol. Rapid Commun. 33 (2012) 2062–2091.
[33] A.I. Rusanov, Micelle Formation in Surfactant Solutions, Chemistry, St. Petersburg, 1992.
[34] V. Sharma, M. Borse, V. Aswal, Synthesis, characterization, and SANS studies of novel alkanediyl-α, ω-bis(hydroxyethylmethylhexadecylammonium bromide) cationic gemini surfactants, J. Colloid Interface Sci. 277 (2004) 450–455.
[35] W. Tong, Q. Zheng, Sh. Shao, Q. Lei, W. Fang, Critical micellar concentrations of quaternary ammonium surfactants with hydroxyethyl substituents on headgroups determined by isothermal titration calorimetry, J. Chem. Eng. Data 55 (2010) 3766–3771.
[36] A.B. Mirgorodskaya, E.I. Yatzkevich, S.S. Lukashenko, L.Ya. Zakharova, A.I. Konovalov, Solubilization and catalytic behavior of micellar system based on gemini surfactant with hydroxyalkylated head group, J. Mol. Liq. 169 (2012) 106–109.
[37] A.Z. Naqvi, G.A. Aldahbali, M. Akram, Kabir-ud-Din, Adsorption and micellization behavior of cationic surfactants (gemini and conventional) — amphiphilic drug systems, J. Solut. Chem. 42 (2013) 172–189.
[38] I. Aiad, M.M. El-Sukkary, E.A. Soliman, M.Y. El-Awady, S.M. Shaban, Characterization, surface properties and biological activity of new prepared cationic surfactants, J. Ind. Eng. Chem. 20 (2014) 1633–1640.
[39] M. Prasad, S.P. Moulik, A. MacDonald, R. Palepu, Self-aggregation of alkyl (C10-, C12-, C14- and C16-) triphenyl phosphonium bromides and their 1:1 molar mixtures in aqueous medium: a thermodynamic study, J. Phys. Chem. B 108 (2004) 355–362.
[40] M.J. Rosen, J.T. Kunjappu, Surfactants and Interfacial Phenomena, 4th Edition John Wiley & Sons Ltd., New York, 2012.
[41] L.Ya. Zakharova, R.R. Kashapov, T.N. Pashirova, A.B. Mirgorodskaya, O.G. Sinyashin, Self-assembly strategy for the design of soft nanocontainers with controlled properties, Mendeleev Commun. 26 (2016) 457–468.
[42] H. Schott, Solubilization of a water-insoluble dye as a method for determining micellar molecular weights, J. Phys. Chem. 70 (9) (1966) 2966–2973.
[43] M.H. Alimohammadi, S. Javadian, H. Gharibi, A.R. Tehrani Bagha, M.R. Alavijeh, K. Kakaei, Aggregation behavior and intermicellar interactions of cationic Gemini surfactants: effects of alkyl chain, spacer lengths and temperature, J. Chem. Thermodyn. 44 (1) (2012) 107–115.
[44] M. Pisárčik, F. Devínsky, M. Pupák, Determination of micelle aggregation numbers of alkyltrimethylammonium bromide and sodium dodecyl sulfate surfactants using time-resolved fluorescence quenching, Open Chem. 13 (2015) 922–931.
[45] B. Tang, Y. Yang, G. Wang, Zh. Yao, L. Zhang, H.-C. Wu, A simple fluorescent probe based on a pyrene derivative for rapid detection of protamine and monitoring of trypsin activity, Org. Biomol. Chem. 13 (32) (2015) 8708–8712.
[46] Y. Qiao, Z. Yao, W. Ge, L. Zhang, H.-C. Wu, Rapid and visual detection of heparin based on the disassembly of polyelectrolyte-induced pyrene excimers, Org. Biomol. Chem. 15 (12) (2017) 2569–2574.
[47] G.P. Drummen, Fluorescent probes and fluorescence (microscopy) techniques-illuminating biological and biomedical research, Molecules 17 (12) (2012) 14067–14090.
[48] J.R. Lakowicz, Principles of Fluorescence Spectroscopy, Springer Science, New York, 2006.
[49] K. Kalyanasundaram, J.K. Thomas, Environmental effects on vibronic band intensities in pyrene monomer fluorescence and their application in studies of micellar systems, J. Am. Chem. Soc. 99 (1977) 2039–2044.
[50] E.D. Goddard, N.J. Turro, P.L. Kuo, K.P. Ananthapadmanabhan, Fluorescence probes for critical micelle concentration determination, Langmuir 1 (3) (1985) 352–355.
[51] E.P. Zhiltsova, T.N. Pashirova, R.R. Kashapov, N.K. Gaisin, O.I. Gnezdilov, S.S. Lukashenko, A.D. Voloshina, N.V. Kulik, V.V. Zobov, L.Ya. Zakharova, A.I. Konovalov, Alkylated 1,4-diazabicyclo[2.2.2]octanes: Self-association, catalytic properties, and biological activity, Russ. Chem. Bull. 61 (1) (2012) 113–120.
[52] E.F. Palermo, D.-K. Lee, A. Ramamoorthy, K. Kuroda, Role of cationic group structure in membrane binding and disruption by amphiphilic copolymers, J. Phys. Chem. B 115 (2011) 366–375.
[53] A.B. Mirgorodskaya, F.G. Valeeva, D.R. Gabdrakhmanov, L.V. Mustakimova, L.Ya. Zakharova, O.G. Sinyashin, V.A. Mamedov, Novel quinoxaline derivative: solubilization by surfactant solutions and membranotropic properties, Tetrahedron 73 (2017) 5115–5121.
[54] R. Hartkamp, T.C. Moore, C.R. Iacovella, M.A. Thompson, P.A. Bulsara, D.J. Moore, C. McCabe, Investigating the structure of multicomponent gel-phase lipid bilayers, Biophys. J. 111 (2016) 813–823.